Improvement and Validation of THUMSv4.1 AM50 Face Model in Virtual Performance Solution and Development of Model Specific Facial Fracture Criteria

Debasis Sahoo, Giacomo Marini

Abstract The present study aimed to improve the finite element (FE) facial bones of THUMSv4.1 in Virtual Performance Solution occupant model. Nose, vomer, nasal septa and ethmoid junctions were modelled to improve the anatomical accuracy of the model. The mesh of nasal complex, nasal bone, maxilla, mandible and zygomatic bones was refined based on convergence study to improve the stability of original model. Material models were assigned to the newly created parts based on literature data. The improved face model was then validated for several impact tests for zygomatic, mandible, maxilla and nasal bone. A CORA Score > 0.85 was obtained for all validations. Further, 191 experimental impact tests on different parts of face bone were replicated with the updated face model. Survival analysis was used to develop model-specific injury risk functions for zygomatic, mandible, maxilla and nasal bone. The proposed face fracture injury risks were based on internal energy at element level.

Keywords Face injury criteria, Finite element head modeling, Face trauma simulation, Survival analysis, Injury tolerance limit.

I. INTRODUCTION

Facial injuries contribute a significant portion of head injuries. Within all injuries sustained in road accidents, facial injuries account for about 36.5% [1]. The global occurrence of facial fractures was approximately 10.7 million cases in 2019 according to the Global Burden of Disease (GBD) [2]. The leading causes of facial injuries include assaults (44–61%), traffic accidents (15.8%), and falls (15%) [3-4]. The human face is composed of several bones that form the structure and provide support for facial features. The facial bones commonly fractured during motor-vehicle crashes are mandible, maxilla, zygomatic and nasal bones. Based on the distribution of facial fractures in frontal impacts within NASS-CDS, the nasal bone is the most frequently fractured facial bone (49%) followed by mandible (18%), maxilla (13%) and zygoma (4%) [5]. According to the Abbreviated Injury Scale (AIS), fractures of facial bones are typically classified as minor or moderate ranging from AIS1 (for nasal bone fracture) to AIS2 (fracture to maxilla, zygoma and mandible) [6]. However, the personal impact of facial injuries is significant due to the long-term cosmetic effects.

Over the last decades, several investigations have been conducted to understand the injury mechanism of facial fractures to mitigate the injury and development of tolerances for major facial bones [7–11]. Impact experiments on the face of unembalmed post-mortem human subjects(PMHS) were conducted with cylindrical or rectangular rigid impactors. The impact force and associated penetration were measured to assess the fracture tolerance of nasal, mandible, zygomatic and maxilla bones. However, conducting classical testing on PMHS has several limitations and can lead to ethical issues. Finite Element (FE) head models offer the possibility to extract complex parameters (e.g. local strain), offering a more accurate description of the injury mechanisms. However, there is a lack of studies available regarding the assessment of facial fracture in FE head model [12–17]. A multilevel validation of facial bones along with development of model-based injury criteria is necessary to predict facial bone fracture accurately in real-world face trauma scenarios.

The head model used in the present study was derived from the 50th percentile male Keysight Technologies Virtual Performance Solution (VPS) THUMS v 4.1 occupant model. Mesh and materials were updated to improve the biofidelity response and the stability of the original model. Based on convergence study, the face bones mesh was refined. A proper nasal complex was modelled. Impact experiments were reproduced with the improved

D. Sahoo (e-mail: debasis.sahoo@volkswagen.de; tel: +49 15229200124) is a safety engineer at VW, Wolfsburg, Germany; the present study was conducted when employed at VAIVA, Gaimersheim, Germany. G. Marini is a safety engineer at Audi, Ingolstadt, Germany.

model for the validation of nasal bone, zygomatic bone, mandible bone and maxilla bone. The updated head model was then used to replicate different kinds of trauma obtained from 191 experiments on different facial bones. Survival analysis was used to develop model specific injury risk functions to predict face bone fractures.

II. METHODS

A brief description about the enhanced THUMS v4 head model (eTHUMSv4_HM) was presented in the first section along with the improvements applied to enhance the biofidelity of the FE face model. Furthermore, a description of the experimental data for FE face model validation and statistical analysis to develop model-based injury criteria for different facial bone fractures were presented.

Enhanced THUMS v4 Head Model

The eTHUMSv4_HM used for this study was based on the head model of THUMSv4.1 AM50 [18]. Details of the original THUMSv4.1 AM50 model were presented by [12–13]. The development of eTHUMSv4_HM was described in [14][19]. The original mesh of the skull and skin were refined to improve the fracture response based on a convergence study conducted for different mesh configurations [14]. To improve brain behavior, a hyper-viscoelastic material which is a combination of Ogden law for hyperelasticity and a Prony series for viscoelasticity model was implemented under VPS platform. Bridging veins were modelled as bar element between superior sagittal sinus, shared with skull nodes. The eTHUMSv4_HM is validated for local brain motion and intracranial pressure data from post-mortem human subjects (PMHS) experiments. The skull model was validated against PHMS head drop tests from [20].

The face bones and nasal complex of the original model is shown in Fig. 1 (A) which are composed of maxilla, zygomatic, mandible, ethmoid, sphenoid, nasal, vomer. However, the ethmoid, sphenoid and vomer were modelled with 2D shell elements. To improve the fracture response and load bearing in frontal impact, the mesh of these bones was updated to two layers of solid hexa elements as in Fig.1 (B). A convergence study was conducted with different mesh configurations for the nasal complex. The reaction force, von Mises stress, hourglass energy and internal energy were compared between the different models. Impactor test simulations were used to investigate the optimal mesh. For facial bones (maxilla, zygomatic, mandible and nasal bone) mesh convergence studies were also conducted. Meshes ranged between two and eight layers of elements. Reaction force, plastic strain, von Mises stress and internal energy were compared for different mesh configurations. A nose modelled with nasal septa and skin was incorporated in the model to improve the bio-fidelity in different impact scenarios as shown in Fig.1 (B). The anthropometry for the nose and septa bone was obtained from [21-22]. The material model for nasal cartilage was obtained from [23–24].

The material parameters for different facial structure are reported in in TABLE I and are based on different studies [17-18] [23-24] [28-29]. All other model parameters, including material cards (except those listed in Table AI), remain unchanged from the original THUMSv4.1 model [18] as implemented in VPS.

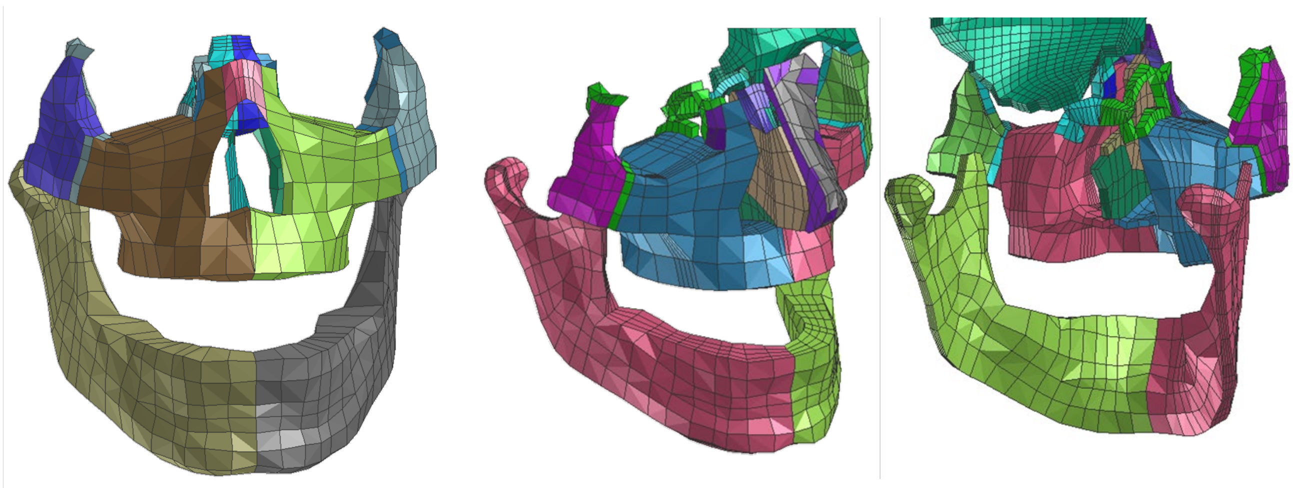

(A) (B)

Fig. 1. Overview of original (A) and improved (B) THUMS v4.1 face and nasal complex

TABLE I
MATERIAL PROPERTIES FOR DIFFERENT PARTS OF FACE FE MODEL

	Young's modulus E (GPa)	Poisson's ratio	Reference
Facial bone Cortical	12.13 ± 2.89	0.22	[17-18], [28-29]
Facial bone Trabecular	1.748 ± 1.41	0.23	[17-18], [28-29]
Teeth	0.00528	0.22	[17-18], [28-29]
Nasal Cartilage	0.00347 ± 0.00026	0.3	[23-24]
Scalp	0.01623 ± 0.00491	0.42	[17-18], [28-29]

Experimental Data for FE Face Model Validation

Impact experiments on the face of 11 unembalmed PMHS were conducted with a cylindrical (25 mm, mass 32/64 kg) impactor by Nyquist *et al.* [7]. The age and mass of the PMHS ranges from 43-66 years and 53-92 kg respectively. The impactor was propelled to the face of the PHMS in anterior-posterior direction with a contact velocity between 10 to 26 km/h. The longitudinal axis of the impactor was at the same elevation as the infraorbital margins of the cadaver skull. Uniaxial accelerometers were attached to the impactor and to the occiput of the PMHS head to analyse the dynamics of the head impacts. Applied force and associated penetration of the impactor to the face data were collected. Each specimen underwent one impact test and nasal bone fractures were observed in each test. Some tests resulted in one or more fractures to zygoma, maxilla and sphenoid bone. It was observed that a peak force of 3kN is a reasonable threshold for a more severe fracture pattern.

Allsop *et al.* [8] performed impact tests on PMHS heads to analyse the deformation response of the zygomatic (eight experiments) and maxilla (six experiments) bones. They used fifteen unembalmed PMHS heads (aged between 39 and 84 years), which were positioned facing upwards in custom-molded plaster foundations. A semi-circular impactor rod weighing 14.5 kg was dropped from heights ranging from 305 to 610 mm onto the zygomatic and maxillary regions. Impacts to the zygomatic and maxillary bones were delivered 10 mm below the suborbital ridge and 10 mm below the anterior nasal spine, respectively. Force and displacement data were recorded at a frequency of 5 kHz.

Cormier *et al.* [9] conducted series of impact experiments on PMHS head with a free-falling rigid aluminum impactor of 3.2 kg with a steel tip along with the use of acoustic emission sensors to determine the time of fracture onset. The impacts were on nasal, maxilla and mandible bones. All heads were frozen and thawed prior to testing. To determine the tolerance of nasal bone to blunt impact a total of 25 male subjects (age range 43 to 76 years) were included in the study. The peak force during each impact ranged from 715 to 2260 N with nasal bone fracture observed in 23 cases. A total of 24 male subjects (age range 43 to 76 years) were used to study the response of maxilla bone by performing 38 impact tests on the sub-nasal region of the maxilla. The peak force ranged from 644 to 2609 N with a pulse duration of each impact ranged from 10 to 15 ms. A facial fracture was produced in 24 tests. The response of mandible bone to blunt impacts was tested by conducting 41 impact tests from 29 PMHS subjects (age range 43 to 76 years). Due to lack of constraint to mandible subsequent motion after initial impact, the force reached an initial peak and then decreased with a secondary peak. The maximum force during the initial peak ranged from 402 to 1607 N.

Bruyere *et al.* [10] performed 15 impact tests on 9 PMHS (age range 58 to 77 years) head, from which 11 tests were on maxilla bones. To replicate the steering wheel rim, a horizontal guided steel cylindrical impactor (diameter equal to 2.25 cm, mass 17 kg) was used. The direction of impact on maxilla or frontal bones was chosen as 30 degrees angled from the mid-sagittal section plane. The impacts are divided into two levels. For low level impacts, the energy ranged between 106 J and 189 J (mean energy 140 J). For high level impacts, the energy ranged between 248 J and 298 J (mean energy 280 J).

Nahum *et al*. [11] conducted several experiments on mandible (17 tests), maxilla (nine tests) and zygoma (25 tests) bones. The impact force was varied by changing the drop height of impactor (circular or flat) with a weight ranging from 1.08-3.82 kg. The range of drop velocity was 2.99 to 5.97 m/s. For eight lateral mandible impacts a flat impactor (area 2.5cm*10cm) was used. The peak force for mandible, maxilla and zygomatic impacts was ranges from 820-4100 N, 625-1980N and 610-3470 N respectively.

The simulation setups for different facial bone impacts were shown in Fig.2. For the validation of nasal bone impact, loading cases 20, 25, 29, 34 and 42 were simulated from Nyquist *et al.* [7]. The velocity of impacts ranged from 3.44-7.14m/s. For zygomatic bone validation, experimental data were taken from eight PMHS tests by Allsop *et al*. [8]. Similarly for mandible and maxilla bones experimental data from Cormier *et al.* [9] and Bruyere *et al*. [10] were used respectively. For mandible, maxilla and zygoma bones response validations, mean loading boundary conditions were applied during the simulations. In all validation cases, the force–displacement or force–time curves generated by the THUMS v4.1 and eTHUMS v4_HM simulations are assessed against the experimental reference data. To quantify the model's performance, the Pearson sample correlation coefficient (r) was used. An r value in the range of 0.1–0.3 signifies poor correlation, while values between 0.5 and 1.0 represent strong consistency between simulation and experimental curves [27]. When corridor bounds were provided for face impact experiments, the CORA (Correlation and Analysis) metric was applied to evaluate the model's predicted face response.

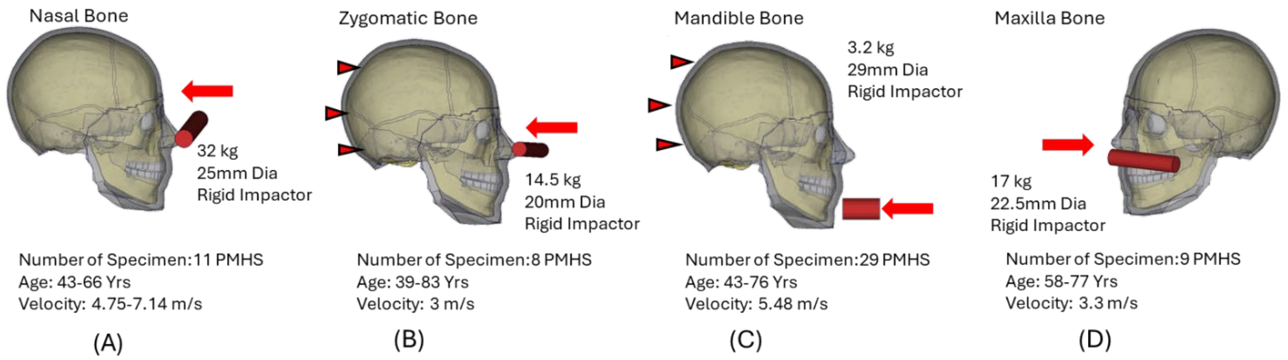

Fig. 2. Simulation setup for nasal (A) [7], zygomatic (B) [8], mandible (C) [9] and maxilla (D) [10] bones

Statistical Method for Development of Injury Criteria

Statistical analyses were carried out for the parameters (e.g. force and internal energy) extracted from the simulation of impact experiments on nose, mandible, maxilla and zygomatic bones to develop model-based face bone fracture criteria. Among the evaluated parameters, internal energy in VPS is calculated from the accumulated stress–strain work at the integration point level and subsequently assembled to element and part levels. For this study, post-processing was performed using part-level energy outputs.

Receiver operating characteristic (ROC) curves were generated to express the performance of a binary classifier system (injured vs non-injured) as its discrimination threshold is varied. The curve is created by plotting the true positive rate (sensitivity) against the false positive rate (fall-out), which is calculated as 1 minus specificity, across various threshold settings. The area under the ROC (AUROC) curve serves as another metric for evaluating test performance. A test is considered 100% accurate if the AUROC is 1, meaning both sensitivity and specificity are 1.0 (no false positives or false negatives). Conversely, a test that fails to distinguish between normal and abnormal results in a diagonal line from (0, 0) to (1, 1), with an AUROC of 0.5. As noted in [25], AUROC values typically range from 0.5 to 1.0. Therefore, the candidate parameter with the highest AUROC value is the best predictor of injury. Also the 95% confidence interval (CI) for AUROC value was include to show the robustness of the study.

Binary injury data (fracture vs. no fracture) were obtained from PMHS impact experiments for different facial regions (nose, mandible, maxilla, and zygomatic bones). Regarding AIS category mapping, this study follows the established definitions provided in the AIS code book [6]. Facial bone fractures are generally categorized as minor to moderate injuries. Accordingly: nasal bone fractures are classified as AIS 1 (minor injury) and fractures of the maxilla, zygoma, and mandible are classified as AIS 2 (moderate injury).

Simulation extracted parameters were then statistically correlated with the experimental injury outcomes. The injury risk curves were derived using survival analysis of binary data, assuming a Weibull distribution (Eq. 1). The survival analysis was performed with the open-source statistical software R (R Project for Statistical Computing). This approach involved fitting a regression model to various potential injury predictors. The probability of face fracture AIS2+ injury is defined by Equation 1:

$$P\,(x) = 1 - e^{-\left(\frac{x}{b}\right)^{a}} \qquad (1)$$

where a is the shape parameter and b is the scale parameter that characterise the Weibull distribution.

III. RESULTS

Face Model Improvement and Validation

Different mesh configurations were used in a simple frontal impact simulation for the convergence study of nasal complex. The reaction force, von Mises stress, hourglass energy and internal energy was compared for different mesh configuration to obtain the optimal mesh as shown in Fig.3. For force (Fig.3 A), von Mises stress (Fig.3 B) and internal energy (Fig.3 D), the green line shows the parameters are converging to a plateau and no further mesh layer required in order not to increase the computation time. The final geometry was based on mesh configuration four with a least hourglass energy among all configurations. Similarly for nasal, mandible, maxilla and zygomatic bones convergence study was conducted with meshes ranging between two and eight layers of element. Force, plastic strain, von Mises stress and internal energy were compared for different mesh layers as shown in Fig. 4. The green curve indicates that the solution is approaching a steady plateau, suggesting that additional mesh layers would not provide meaningful improvements and would only increase computation time unnecessarily. The convergence study showed that four layers of trabecular delivered the optimum response.

The nasal bone is validated against cylindrical impactor impact experimental data from Nyquist *et al.* [7]. Loading cases 20, 25, 29, 34 and 42 were simulated (for THUMS v4.1 and eTHUMSv4_HM) and force-displacement data were compared with experiments as shown in Fig. 5.A. The experimental and simulation curves are in black, red (THUMS v4.1) and blue (eTHUMSv4_HM) color respectively. A good agreement was found between eTHUMSv4_HM simulations and experimental curve (average r > 0.881). For THUMS v4.1 simulation data average correlation of r=0.562 was obtained against experimental data. Additionally, acceleration comparisons between simulation result and experimental data for both the impactor and occipital regions across these five tests have been added to the Appendix Fig. A1-A5.

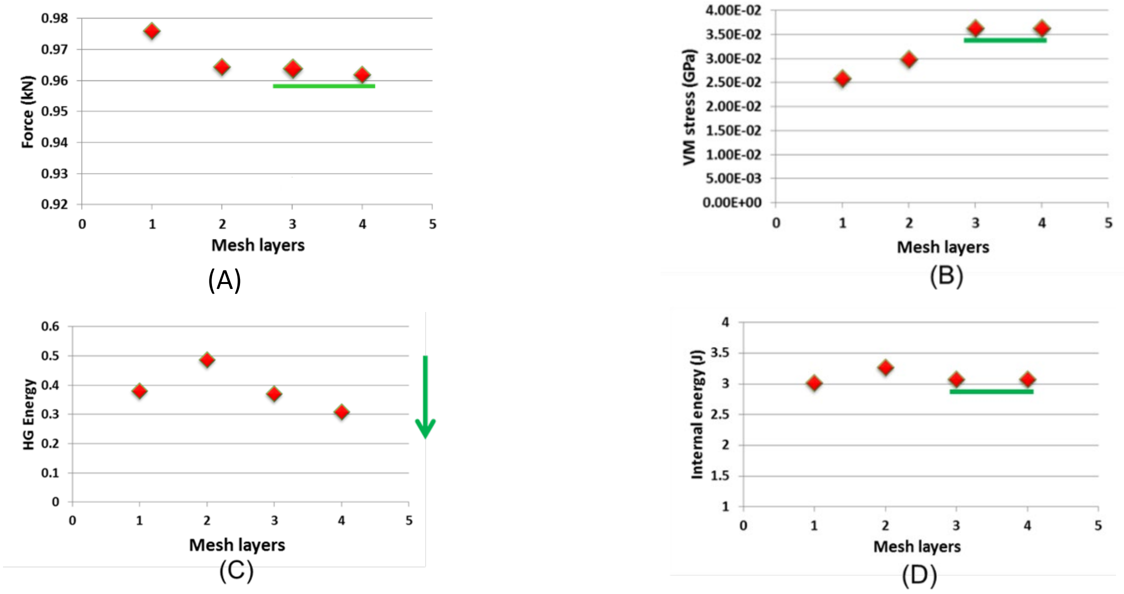

Fig. 3. Results for convergence study for nasal complex. The reaction force (A), von Mises stress (B), hourglass energy (C) and internal energy (A) was compared for different mesh configuration.

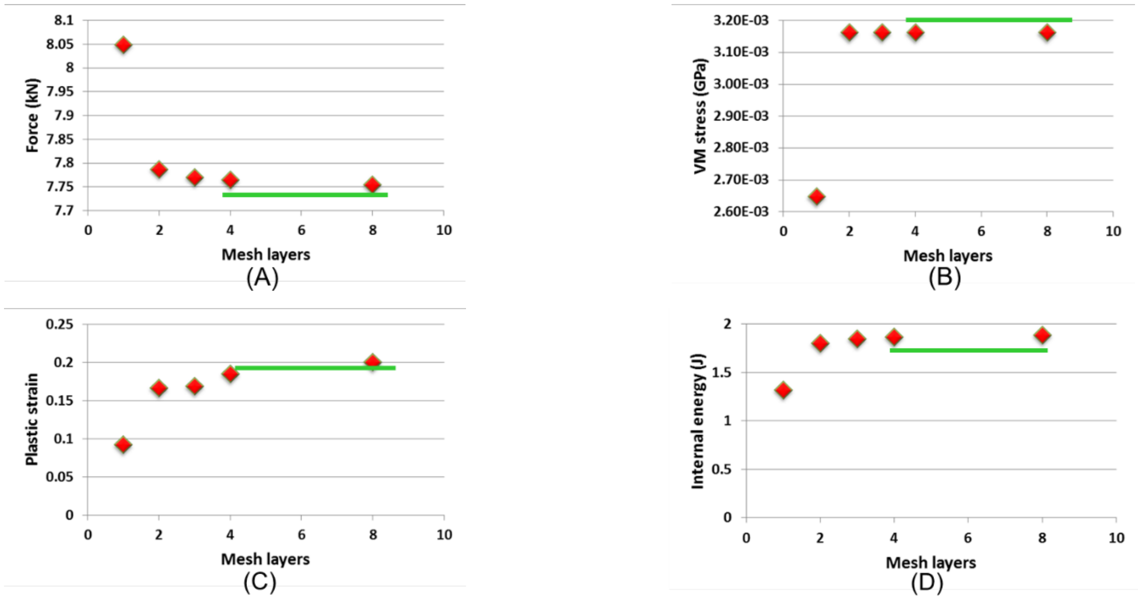

Fig. 4. Results for convergence study for face bones. The reaction force (A), von Mises stress (B), Plastic strain (C) and internal energy (A) was compared for different mesh configuration.

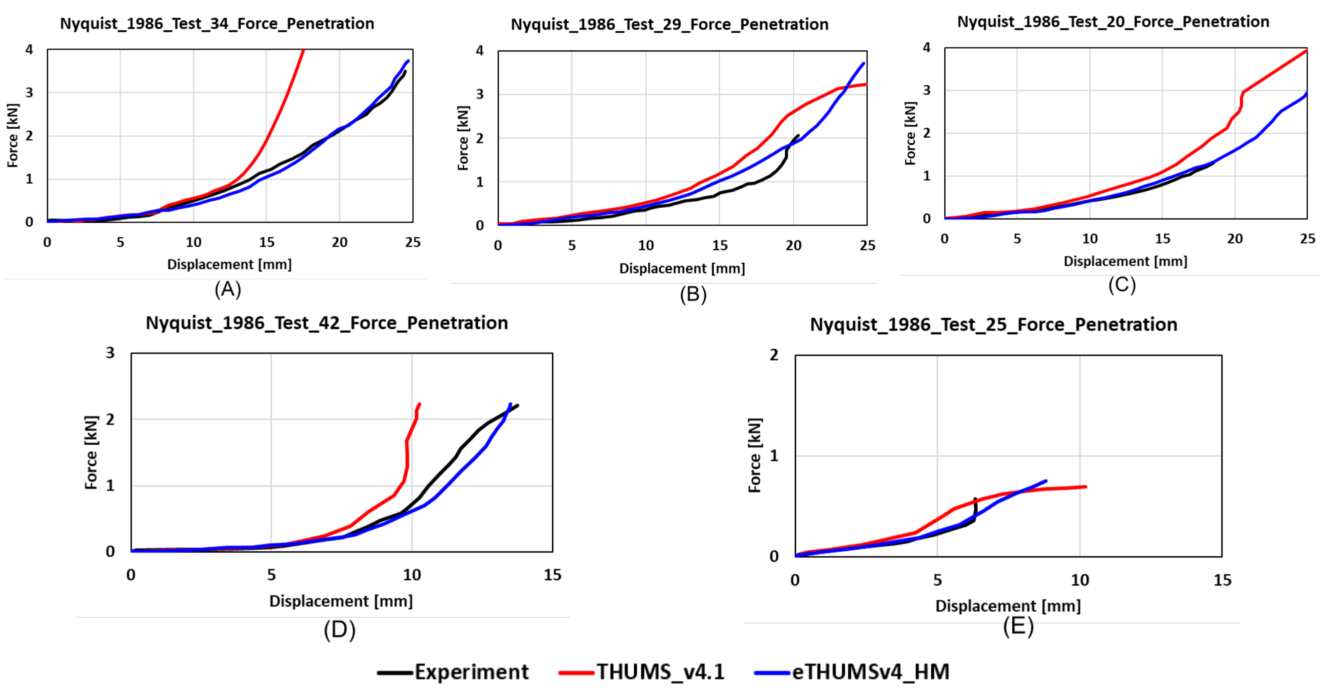

Fig. 5. Validation for nasal bone response for test 20 (A), 29 (B), 34 (C), 42 (D) and 25 (E) from Nyquist *et al*. [7]. Force-displacement plots comparison between simulation result (THUMS v4.1 and eTHUMSv4_HM) and experimental data.

Experimental data from Allsop *et al.* [8] was used for validation of zygomatic bone behavior. The corridor and the mean experimental force displacement curve were obtained from eight impacts tests to PMHS zygomatic bones as shown Fig.6 (A) (black curves). A CORA rating of 0.86 and correlation (r) of 0.9 was obtained when comparing the eTHUMSv4_HM simulation and experimental mean curves. For THUMS v4.1 zygoma validation, a CORA rating of 0.54 and correlation (r) of 0.54 was obtained.

For mandible 41 impact tests are used from Cormier *et al.* [9] to develop the corridors and mean experimental curve as shown in Fig.6. (B) (black curves). A CORA score of 0.842 (and r = 0.75) is observed between simulation and experimental data. For THUMS v4.1 mandible validation, a CORA rating of 0.51 and correlation (r) of 0.61 was obtained.

The experimental corridors based on 11 tests for maxilla bones are shown in Fig. 6. (C) (black curves) from

Bruyere *et al*. [10]. The simulation was conducted for mean energy level and force time data from simulation (in blue) were compared. A CORA rating of 0.851 was obtained for maxilla validation. For THUMS v4.1 maxilla validation a CORA rating of 0.42 was obtained.

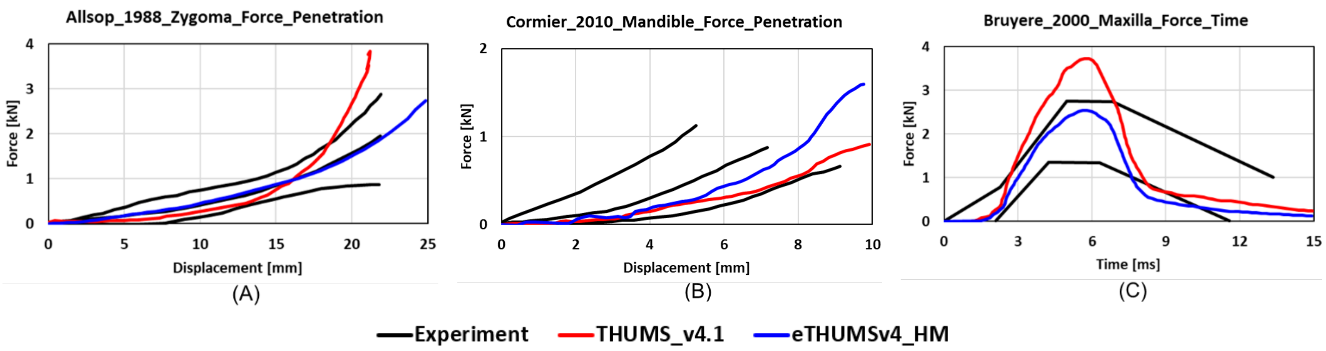

Fig. 6. Validation for zygomatic (A), mandible (B) and maxilla (B) force response against experimental corridor. Force-displacement/time plots comparison between simulation result (THUMS v4.1 and eTHUMSv4_HM) and experimental data.

Face Injury Criteria

A total of 191 experiments were reconstructed to develop model-based injury criteria for facial bones. Potential parameters like force and internal energy were extracted to predict facial bone fracture. For nasal bone 11 tests from Nyquist *et al*. [7] and 25 tests for Cormier *et al*. [9] were simulated. The AUROC for each candidate parameter was computed and nasal bone internal energy was found to have the highest AUROC value of 0.9 (CI: 0.88 & 0.92).

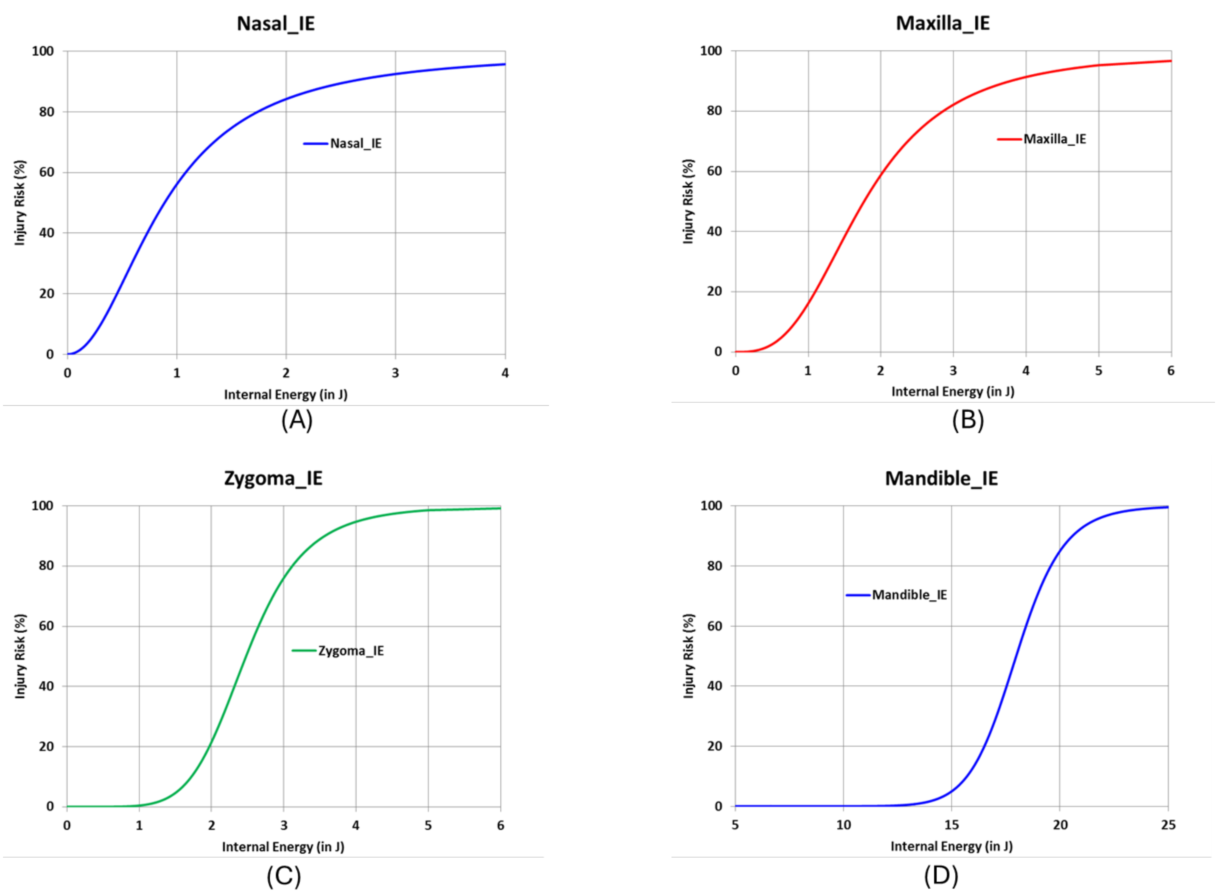

Fig. 7. Injury risk curve to predict nasal (A), maxilla (B), zygomatic (C) and mandible (D) bone fracture by using bone internal energy as injury predictor.

Survival analysis with Weibull distribution was done for binary fractured/non-fractured data for different potential parameters. The injury risk curve to predict nasal bone fracture by considering internal energy as predictor is shown in Fig. 7 (A). Nasal bone fracture is AIS1 injury and the 50% injury risk of nasal bone fracture was reached for an internal energy of 886mJ. For maxilla bone injury criteria 64 (38 Cormier *et al.* [9], six from Allsop *et al*. [8], 11 from Bruyere *et al*. [10] and nine from Nahum *et al.* [11]) impact experiments are reproduced. Maxilla internal energy had the highest AUROC of 0.92 (CI: 0.89 & 0.95). is the predictor of maxilla bone fracture and 50% risk of Maxilla bone fracture is at 1766mJ as shown in Fig. 7. (B). A total of 33 experimental data from Allsop *et al.* [8] and Nahum *et al*. [11] were reconstructed to develop the injury criteria for zygomatic bone. Internal energy of zygoma with AUROC 0.95 (CI: 0.93 & 0.97) was used to predict the fracture and 50% risk of Zygoma bone fracture is at 2477mJ as shown in Fig.7 (C). For mandible, 58 impact data from Cormier *et al.* [9] and Nahum *et al.* [11] were reproduced through simulation with eTHUMSv4_HM. AUROC of 0.97 (CI: 0.96 & 0.98) was obtained for mandible internal energy and 50% risk of Mandible bone fracture is at 17978mJ as shown in Fig.7 (D). As there are only 33 data points for zygomatic bone, to improve the robustness of survival analysis, the 64 data points of maxilla are combined to generate a combined maxilla-zygoma injury risk curve as shown in Fig.8. The AUROC value of combined data is 0.94 (CI: 0.91 & 0.97) for internal energy and 50% risk of combined Maxilla and Zygoma bones fracture is at 2324mJ.

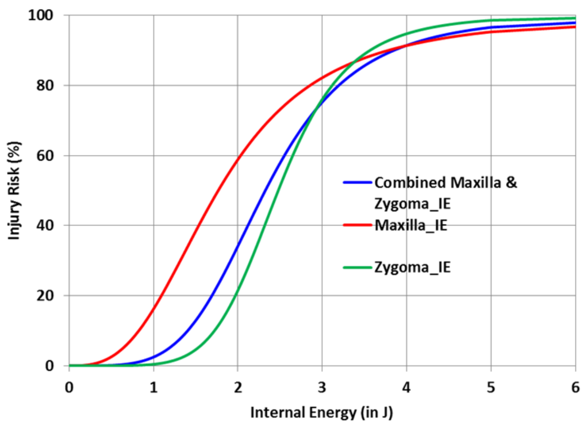

Fig. 8. Combined injury risk curve for maxilla and zygomatic bone by using bone internal energy as injury predictor.

IV. DISCUSSION

The objectives of this study include improvements in facial bone geometry of eTHUMSv4_HM and numerical modelling. In particular, the geometry of nasal complex and nasal, mandible, maxilla and zygomatic bones are refined based on convergence study. A nose modelled with nasal septa and skin was incorporated in the model to improve the biofidelity in different impact scenarios. These updates were then validated against experimental data. The resulting eTHUMSv4_HM was then used to develop model specific facial bone fracture criteria.

The study presented a methodology for validation of facial bones. A very good agreement (r >0.881) between force-displacement data from the simulation of eTHUMSv4_HM and the experiment was achieved during the validation for nasal bone. Five test data 20, 25, 29, 34 and 42 from Nyquist *et al.* [7] were reconstructed for nasal bone validation process. These five experiments took into account different levels of impact velocities. For mandible and zygoma validation the simulation force-displacement data was compared with mean experimental data with CORA rating of 0.86 and 0.842 respectively. For maxilla bone the simulation curve was within the force-time corridor of experimental data with a CORA score of 0.851. An average correlation (r) value more than 0.85 was observed during the validation of facial bones.

Despite extensive developments in human body modeling, there remains a notable lack of dedicated validation studies focusing specifically on FE facial models [17] [26] [30-31]. Most existing research emphasizes whole-head or whole-body validation, with head response typically assessed only indirectly through global head kinematics or intracranial metrics. The current study extensively validated the facial bones of eTHUMSv4_HM compared to the other studies in literature and commercial head models from GHBMC and SAFER [12] [16–17] [26] [30-31]. In comparison, the facial model validation of GHBMC head model typically limited to fewer Nyquist

[7] and Allsop [8] test cases [30]. The original THUMS 4.1 head model is limitedly validated for facial bones [12-13]. Similarly, the SAFER HBM relies on whole-body and kinematic validation using PMHS data, focusing on head trajectory and acceleration responses, but does not include dedicated facial validation using force–displacement corridors or specific cadaver facial impact datasets [31]. The current model is validated for most numbers of tests from Nyquist [7] and not only compared with force-displacement data but also acceleration plots for impactor and occipital of head. Furthermore, the model is validated against multiple independent cadaver datasets, including Allsop et al. [8], Cormier et al. [9], and Bruyère et al. [10], demonstrating that the simulated responses consistently fall within experimental corridors and accurately reproduce mean experimental trends. This multi-dataset, face-specific validation goes beyond the scope of most existing HBMs.

Model predictions are not governed solely by material parameters. The conducted mesh convergence study shows that geometry and mesh (e.g., trabecular bone layering) also significantly affect internal energy absorption and contact forces. This highlights that the validity of the simulations arises from a combined effect of material modeling, geometry, and mesh fidelity, rather than material properties alone.

A total of 191 experimental facial impact tests were reconstructed to develop injury criteria specific to the eTHUMSv4_HM. Force and internal energy were extracted for each simulation and based on statistical analysis best candidate parameter to predict facial bone fracture was chosen. Bone internal energy has the highest AUROC value in all cases and provided the highest correlation with the occurrence of AIS1/AIS2 injury sustained to the facial bone. Previous studies also demonstrated that bone internal energy is a suitable predictor of bone fracture mechanisms [14][15]. Nasal bone fracture is AIS1 injury and the 50% injury risk of bone fracture was reached for an internal energy of 886mJ. Maxilla, zygomatic and mandible bone fractures are AIS2 injury, and the 50% injury risks are 1766mJ, 2477mJ and 17978mJ respectively. The higher energy required needed to induce a fracture of the mandible is in accordance with [9][11]. The AIS levels were assigned directly based on the anatomical location of the experimentally observed fractures. Therefore, the developed injury risk curves represent the probability of sustaining region-specific fracture injuries mapped to their respective AIS severity levels.

The confidence of survival analysis is influenced by the sample size. In the current study a total of 191 face trauma cases were replicated. However, for the zygomatic bone only 33 data points were available. To improve the robustness of the survival analysis, the 64 data points of maxilla were combined to generate a combined maxilla-zygoma injury risk curve. The AUROC value of combined zygomatic and maxilla data is 0.94 for internal energy and 50% risk of combined Maxilla and Zygoma bones fracture is at 2324mJ.

The current study has been developed for a modified VPS version of the THUMSv4.1 50th percentile HBM head model. Although the approach for developing the injury risk criteria can generally be applied to other HBMs, the use of internal energy as injury predictor needs to be confirmed. Furthermore, with regard to HBMs which are developed in different FE solver environments, the computation of the internal energy at element level could be different. Therefore, the authors would recommend to avoid applying directly the proposed injury risk criteria to other HBMs without ensuring the harmonization between HBMs and their outcomes.

The current study focuses on the improvement of the eTHUMSv4_HM and on the development of fracture criteria for facial bones based on 50% adult male anthropometry. Variations in specimen mass and geometry were not considered during reconstruction, which may potentially affect the accuracy of the injury risk functions when applied beyond the standard 50th percentile adult male population.

V. CONCLUSION

The eTHUMSv4_HM was further improved for nasal complex and mesh of facial bones. The enhanced FE face model was validated against several experimental impact tests. A high correlation (r > 0.75 and CORA > 0,84) between experimental data and simulations was obtained during the validation of nasal, mandible, zygomatic and maxilla bones. The improved face model represents a significant improvement with respect to the original THUMS v4.1 (r < 0,61 and CORA < 0,54) face model. The incorporation of the nasal complex might improve the ability to have a realistic interaction with the restraint system and allow the investigation of new customer functions. Furthermore, model specific injury risks functions were developed for fracture of nasal bone, zygomatic bone, mandible bone and maxilla bone with internal energy as the predictor. The present study is the first to develop detailed individual fracture criteria for facial bones for VPS THUMS v4.1 AM50 human body model.

VI. ACKNOWLEDGEMENTS

The authors would like to acknowledge AUDI AG for funding this study.

VII. REFERENCES

[1] Gururaj, G. (2002) Epidemiology of traumatic brain injuries: Indian scenario. Neurological Research, **24**(1): pp.24–28.

[2] GBD 2019 Fracture Collaborators (2021) Global, regional, and national burden of bone fractures in 204 countries and territories, 1990–2019: a systematic analysis from the Global Burden of Disease Study 2019. The Lancet Healthy Longevity, **2**(9): pp.e580–e592.

[3] Ludi, E. K., Rohatgi, S., Zygmont, M. E., Khosa, F., Hanna, T. N. (2016) Do radiologists and surgeons speak the same language? A retrospective review of facial trauma. American Journal of Roentgenology, **207**(5): pp.1070–1076.

[4] Lee, K. H. (2009) Interpersonal violence and facial fractures. Journal of Oral and Maxillofacial Surgery, **67**(9): pp.1878–1883.

[5] Cormier, J., Duma, S. (2009) Epidemiology of facial fractures in automotive collisions. Annals of Advances in Automotive Medicine, **53**: pp.169–176.

[6] Abbreviated injury scale, update 2015, Copyright, 2015, Association for the Advancement of Automotive Medicine, Barrington, IL, USA.

[7] Nyquist, G. W., Cavanaugh, J. M., Goldberg, S. J., King, A. I. (1986) Facial impact tolerance and response. Proceedings of the 30th Stapp Car Crash Conference, 1986, San Diego, USA.

[8] Allsop, D. L., Warner, C. Y., Wille, M. G., Scheider, D. C., Nahum, A. M. (1988) Facial impact response: a comparison of the Hybrid III dummy and human cadaver. Proceedings of the 32nd Stapp Car Crash Conference, 1988, Atlanta, USA.

[9] Cormier, J., *et al.* (2010) Biomechanical response of the human face and corresponding biofidelity of the FOCUS headform. SAE International Journal of Passenger Cars – Mechanical Systems, **3**(1): pp.842–859.

[10] Bruyère, K., Bermond, F., Bouguet, R., Caire, Y., Ramet, M., *et al.* (2000) Human maxilla bone response to 30 degree oriented impacts and comparison with frontal bone impacts. Proceedings of the 44th Association for the Advancement of Automotive Medicine Conference, 2000, Chicago, USA.

[11] Nahum, A. M. (1975) The biomechanics of facial bone fracture. The Laryngoscope, **85**(1): pp.140–156.

[12] Atsumi, N., Nakahira, Y., Iwamoto, M. (2016) Development and validation of a head/brain FE model and investigation of influential factors on the brain response during head impact. International Journal of Vehicle Safety, **9**(1): pp.1–23.

[13] Iwamoto, M., Atsumi, N., Nakahira, Y., Hirabayashi, S. (2016) Development of human head/brain FE model with material modeling of brain parenchyma and its application to investigation on head rotational injury mechanism. Proceedings of the 6th International Symposium on Human Modeling and Simulation in Automotive Engineering, 2016, Heidelberg, Germany.

[14] Sahoo, D., Jani, D., Marini, G. (2024) Validation of THUMSv4.1 head model in Virtual Performance Solution and development of model-specific head injury criteria: skull fracture, mild diffuse axonal injury and subdural haematoma. Proceedings of the IRCOBI Conference, 2024, Stockholm, Sweden.

[15] Sahoo, D., Deck, C., Yoganandan, N., Willinger, R. (2016) Development of skull fracture criterion based on real-world head trauma simulations using finite element head model. Journal of the Mechanical Behavior of Biomedical Materials, **57**: pp.24–41.

[16] Zhang, L., Yang, K., Dwarampudi, R., Omori, K., Li, T., *et al.* (2001) Recent advances in brain injury research: a new human head model development and validation. Stapp Car Crash Journal, **45**: pp.369–394.

[17] Mao, H., *et al.* (2013) Development of a finite element human head model partially validated with thirty-five experimental cases. Journal of Biomechanical Engineering, **135**(11): p.111002.

[18] Toyota Motor Corporation Toyota Central R&D Labs, Inc., Biomechanics Laboratory, Mechanical Engineering Department II, Nagakute, Japan, https://www.toyota.co.jp/thums/.

[19] Sahoo, D., Coulongeat, F., Fuerst, F., Marini, G. (2020) Comparison of head injury criteria based on real-world accident simulations under Virtual Performance Solution. Proceedings of the IRCOBI Conference, 2020, Munich, Germany.

[20] Sahoo, D., Deck, C., Yoganandan, N., Willinger, R. (2013) Anisotropic composite human skull model and skull fracture validation against temporo-parietal skull fracture. Journal of the Mechanical Behavior of Biomedical Materials, **28**: pp.340–353.

[21] Young, J. W. (1993) Head and face anthropometry of adult U.S. civilians. Report DOT/FAA/AM-93/10, Federal Aviation Administration, Washington DC, USA.

[22] Kim, J. H., Jung, D. J., Kim, H. S., Kim, C. H., Kim, T. Y. (2014) Analysis of the development of the nasal septum and measurement of the harvestable septal cartilage in Koreans using three-dimensional facial bone computed tomography scanning. Archives of Plastic Surgery, **41**(2): pp.163–170.

[23] Griffin, M. F., Premakumar, Y., Seifalian, A. M., Szarko, M., Butler, P. E. (2016) Biomechanical characterisation of the human nasal cartilages; implications for tissue engineering. Journal of Materials Science: Materials in Medicine, **27**(1): p.11.

[24] Westreich, R. W., Courtland, H. W., Nasser, P., Jepsen, K., Lawson, W. (2007) Defining nasal cartilage elasticity: biomechanical testing of the tripod theory based on a cantilevered model. Archives of Facial Plastic Surgery, **9**(4): pp.264–270.

[25] Metz, C. E. (1986) ROC methodology in radiologic imaging. Investigative Radiology, **21**: pp.720–733.

[26] Tse, K. M., Tan, L. B., Lee, S. J., Lim, S. P., Lee, H. P. (2014) Correlation between facial trauma and brain injury – a finite element study. Proceedings of the 15th International Conference on Biomedical Engineering, 2013, Singapore.

[27] Mate, K. K. V., Bushnell, D. M., Anatchkova, M., Martin-Delgado, J., Ahmed, O. M. Y., *et al.* (2022) What is with all these different correlation thresholds? Quality of Life Research, 31(Suppl 1): p.S42.

[28] Kimpara, H., Nakahira, Y., Iwamoto, M., Miki, K., Ichihara, K., Kawano, S. and Taguchi, T. (2006) Investigation of anteroposterior head-neck responses during severe frontal impacts using a brain-spinal cord complex FE model', Proceedings of the 50th Stapp Car Crash Conference, 6–8 November, Dearborn, MI, USA, pp.509–544.

[29] Yang, King & Hu, Jingwen & White, Nicholas & King, Albert & Chou, Clifford & Prasad, Priya. (2006). Development of Numerical Models for Injury Biomechanics Research: A Review of 50 Years of Publications in the Stapp Car Crash Conference. Stapp car crash journal. 50. 429-490.

[30] Lyu D, Zhou R, Lin C, Prasad P and Zhang L (2022) Development and Validation of a New Anisotropic Visco-Hyperelastic Human Head Finite Element Model Capable of Predicting Multiple Brain Injuries. Front. Bioeng. Biotechnol. 10:831595. doi: 10.3389/fbioe.2022.831595.

[31] Lindgren, N., Yuan, Q., Pipkorn, B., Kleiven, S., Li, X. (2023) Development and Whole-Body Validation of Personalizable Female and Male Pedestrian SAFER Human Body Models, https://arxiv.org/abs/2305.13918, accessed Dec. 2023.

VIII. APPENDIX

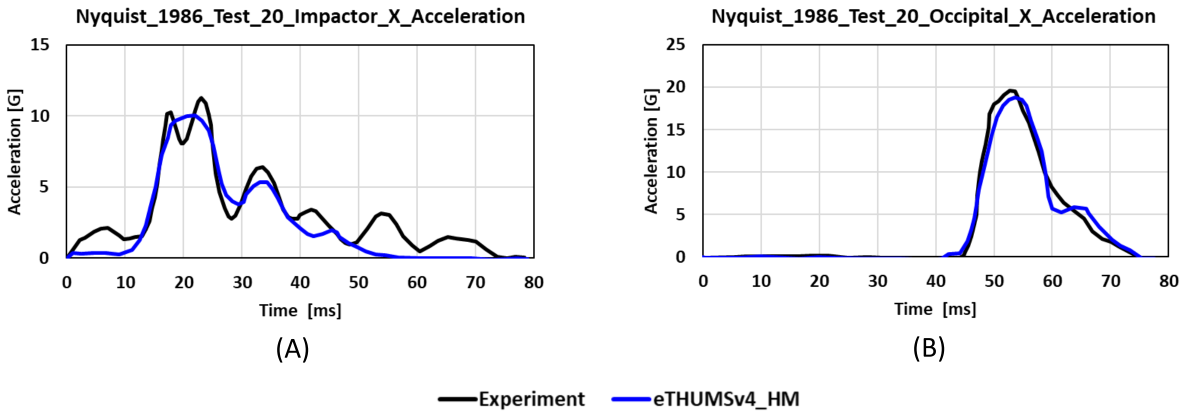

Fig. A1. Comparison of acceleration of impactor (A) and Occipital (B) between experiment (Test 20) and simulation result for eTHUMSv4_HM filtered at 180hz.

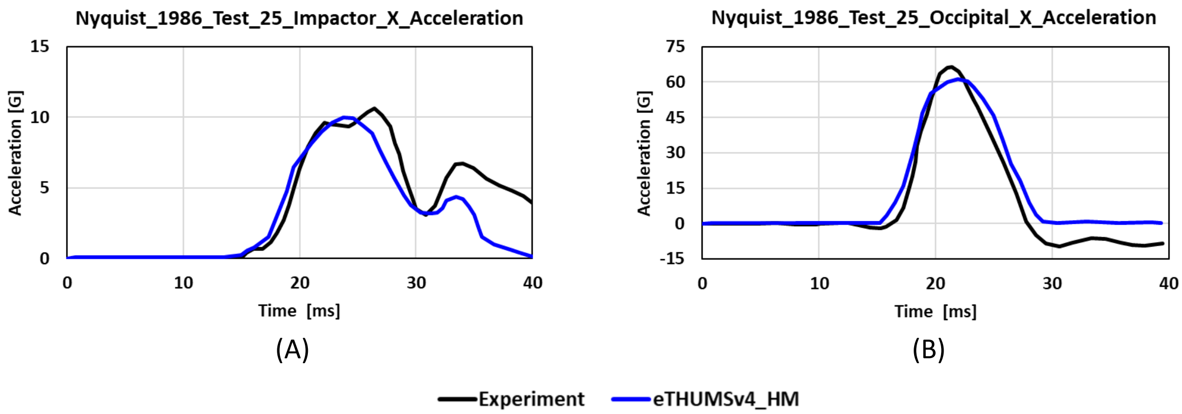

Fig. A2. Comparison of acceleration of impactor (A) and Occipital (B) between experiment (Test 25) and simulation result for eTHUMSv4_HM filtered at 180hz.

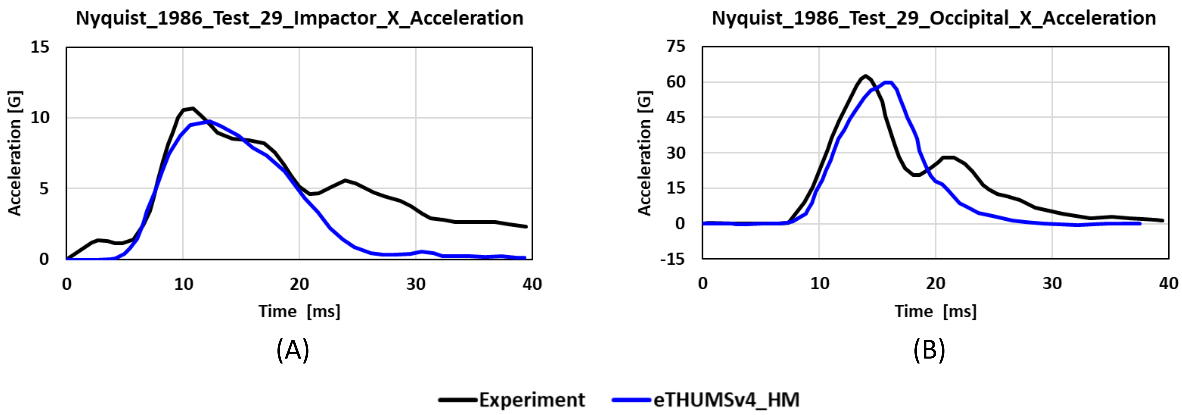

Fig. A3. Comparison of acceleration of impactor (A) and Occipital (B) between experiment (Test 29) and simulation result for eTHUMSv4_HM filtered at 180hz.

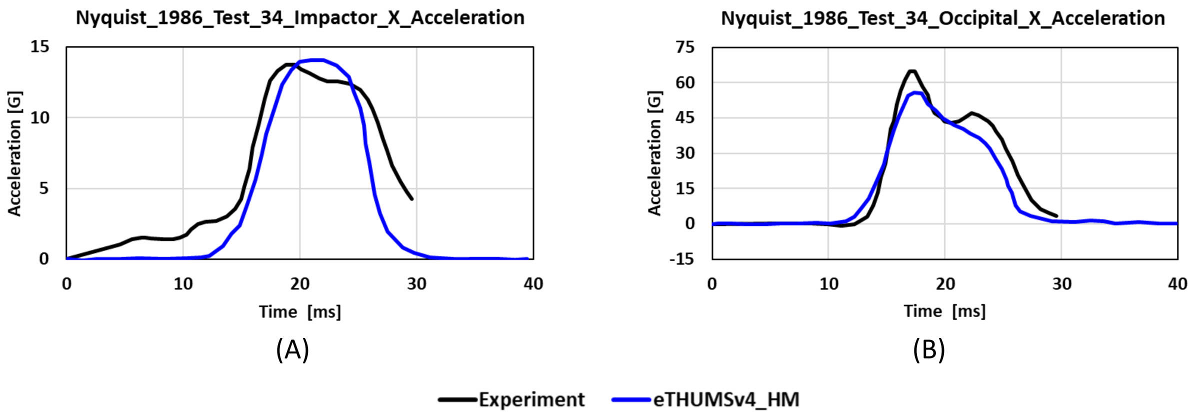

Fig. A4. Comparison of acceleration of impactor (A) and Occipital (B) between experiment (Test 34) and simulation result for eTHUMSv4_HM filtered at 180hz.

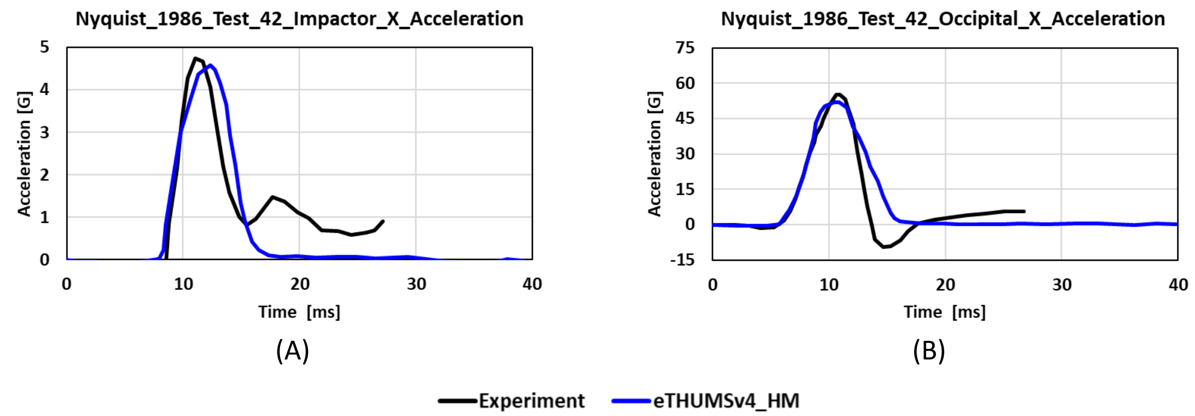

Fig. A5. Comparison of acceleration of impactor (A) and Occipital (B) between experiment (Test 42) and simulation result for eTHUMSv4_HM filtered at 180hz.